HHS Public Access

Author manuscript

*J Invest Dermatol*. Author manuscript; available in PMC 2016 May 01.

Published in final edited form as:

*J Invest Dermatol*. 2015 November ; 135(11): 2742–2752. doi:10.1038/jid.2015.283.

# Lymphatic function regulates contact hypersensitivity dermatitis in obesity

**Ira L. Savetsky, MD**[1,*], **Nicholas J. Albano, BS**[1,*], **Daniel A. Cuzzone, MD**[1], **Jason C. Gardenier, MD**[1], **Jeremy S. Torrisi, BA**[1], **Gabriela D. García Nores, MD**[1], **Matthew D. Nitti, BA**[1], **Geoffrey E. Hespe, BS**[1], **Tyler S. Nelson, BS**[2,3], **Raghu P. Kataru, PhD**[1], **J. Brandon Dixon, PhD**[2,3,4], and **Babak J. Mehrara, MD**[1]

[1]The Department of Surgery, Division of Plastic and Reconstructive Surgery, Memorial Sloan Kettering Cancer Center, New York, NY

[2]Parker H. Petit Institute for Bioengineering and Bioscience, Georgia Institute of Technology, Atlanta, Georgia

[3]George W. Woodruff School of Mechanical Engineering, Georgia Institute of Technology, Atlanta, Georgia

[4]Wallace H. Coulter Department of Biomedical Engineering, Georgia Institute of Technology, Atlanta, Georgia

### Keywords

Obesity; inflammation; lymphatics; dermatitis

## Introduction

It is estimated that more than one third of U.S. adults are obese, with the incidence rapidly rising in adult and pediatric populations (Ogden *et al*., 2014). Obesity is associated with a wide variety of pathologies, including coronary artery disease, insulin resistance, diabetes, and malignancy (Garfinkel, 1985; Glass and Olefsky, 2012; Lavie *et al*., 2009; Mokdad *et al*., 2003). In addition, obesity has a profound impact on a variety of dermatologic diseases, including psoriasis and atopic dermatitis in both children and adults (Marino *et al*., 2004; Silverberg *et al*., 2011; Silverberg *et al*., 2012).



**Correspondence**: Babak J. Mehrara, MD, Member Memorial Hospital, Associate Professor of Surgery (Plastic), Weill Cornell University Medical Center, 1275 York Avenue, Suite MRI 1006, New York, New York, 10065. Tel.: (212) 639-8639; Fax: (212) 717-3677. mehrarab@mskcc.org.

*These authors contributed equally to this manuscript.

**Disclosures**:

BD and TN receive research funding and they and Georgia Tech are entitled to sales royalty from LymphaTech, which is developing products related to the research described in this paper. In addition, BD holds equity in the company. This study could affect their personal financial status. The terms of this arrangement have been reviewed and approved by Georgia Tech in accordance with its conflict of interest policies. The remaining authors state no conflict of interest.

Chronic inflammation is a major mechanism regulating pathological changes in obesity. For example, visceral adipose deposition in obese individuals is associated with chronic infiltration of activated T cells and macrophages. These changes result in increased local and systemic expression of a multitude of inflammatory cytokines, including tumor necrosis factor alpha (TNF-α), interleukin (IL)-6, IL-1β, chemokine ligand 2 (CCL2), and others (Gregor and Hotamisligil, 2011; Lumeng and Saltiel, 2011). These inflammatory changes play crucial roles in the development of metabolic syndrome, insulin resistance, tumor metastasis, and cardiovascular disease (Glass and Olefsky, 2012; Lavie *et al*., 2009; Mokdad *et al*., 2003; Perez-Hernandez *et al*.). Similarly, previous studies have shown that obese patients have increased subcutaneous tissue inflammation and that these pathological changes contribute to the development of dermatological disorders (Gerdes *et al*., 2011; Hamminga *et al*., 2006). However, while it is clear that inflammation is a key regulator of pathological outcomes in obesity, the effects of these changes on dermatological diseases and the regulation of inflammatory responses in obesity remain poorly understood.

Recent studies have shown that obesity impairs lymphatic function both in mice and humans (Arngrim *et al*., 2013; Lim *et al*., 2009; Lim *et al*., 2013; Savetsky *et al*., 2014; Weitman *et al*., 2013). For example, our group has reported that obese mice have decreased ability to transport interstitial fluid via cutaneous lymphatics and have markedly decreased trafficking of antigen presenting cells to regional lymph nodes (Weitman *et al*., 2013). Furthermore, Rutkowski *et al*. demonstrated that adipose tissue accumulation reduces interstitial fluid transport by lowering hydraulic conductivity (Rutkowski *et al*., 2010). Other investigators have shown that obese mice have impaired lymphatic collecting vessel pumping function (Blum *et al*., 2014). These findings are supported by clinical studies demonstrating that obese patients have decreased clearance of macromolecules from fat depots when compared to normal controls, and that massively obese patients spontaneously develop lymphedema (a condition in which impaired lymphatic drainage function results in chronic limb swelling) (Arngrim *et al*., 2013; Greene *et al*., 2012). The relationship between obesity and the lymphatic system appears to be bidirectional since previous studies have shown that mice with congenital lymphatic defects resulting from *Prox-1* haploinsufficiency go on to develop adult onset obesity (Harvey *et al*., 2005). Because the lymphatic system is a critical physiologic regulator of inflammation and immune responses, obesity-induced lymphatic dysfunction may act in a feed forward manner to amplify the pathological consequences of obesity in end organs. This hypothesis is supported by previous studies demonstrating that improving lymphatic function with exogenous delivery of lymphangiogenic cytokines, such as vascular endothelial growth factor (VEGF)-C, decreases acute/chronic skin inflammation in lean mice (Huggenberger *et al*., 2010; Kataru *et al*., 2009). Thus, improving lymphatic function in obese patients may serve as a novel means of mitigating the pathology of cutaneous disorders associated with obesity.

In the current study, we investigated the role of the lymphatic system in regulating dermatitis in obesity. We found that obese mice have impaired lymphatic function and heightened dermatitis responses to inflammatory skin stimuli. Obese mice had both higher peak inflammation and a delayed clearance of inflammatory responses. Increasing lymphatic function by injection of recombinant human VEGF-C (rhVEGF-C) markedly decreased

dermatitis responses in obese mice, leading to decreased peak inflammation and an increased rate of its clearance. Taken together, our findings suggest that obesity-induced changes in the lymphatic system result in an amplified and prolonged inflammatory response in the skin.

## Results

### Obese mice have impaired lymphatic function at baseline

As expected, feeding male C57BL/6J mice a high fat diet (HFD) for 10–12 weeks resulted in a significant increase in body weight and subcutaneous adipose deposition as reflected by increased perilipin-positive cell accumulation and ear thickness when compared with mice fed a normal chow diet (Figure 1a, b, c; $p<0.01$ for both). Consistent with our previous studies, immunofluorescence analysis of ear skin demonstrated significant baseline increases in the number of $CD45^+$ and $CD3^+$ cells in obese mice as compared with lean controls (Figures 1d, e, S1a, b; $p<0.01$ for all) (Savetsky *et al*., 2014; Weitman *et al*., 2013). In addition, obese mice had significantly fewer subcutaneous lymphatic vessel endothelium hyaluronan receptor 1 $(LYVE\text{-}1)^+$ lymphatic vessels as compared with controls (Figure 1d, f; $p<0.01$). Lymphangiography using subdermal Evans blue dye injection demonstrated the presence of leaky capillary lymphatics (white arrows) in obese mice as compared to lean controls (Figure 1g**; upper panel**). These findings were confirmed with functional lymphatic vessel staining using fluorescein isothiocyanate (FITC) fluorescently-conjugated tomato lectin in whole mounted specimens stained for alpha-smooth muscle actin (α-SMA) and LYVE-1. Obese animals had significantly less uptake (yellow arrows) and more extravasation of peripherally injected tomato lectin in the ear (white arrow and outlined region) as compared to controls (Figure 1g**; lower panel**). Furthermore, analysis of collecting lymphatic pumping frequency in the hind limb and tail demonstrated a 2–3 fold decrease in packet frequency (visualized using NIR imaging) in obese mice as compared with controls (Figure 1h **and** Movies S1–4; $p<0.05$ and $p<0.01$ for the tail and hind limb, respectively). Finally, consistent with our observation that obese mice have impaired lymphatic function, we found that obese mice had significantly decreased systemic uptake of peripherally injected macromolecules (FITC-dextran) as compared with controls (Figure S2b; $p<0.05$).

### Obese mice have normal antibody production but impaired T cell recall

Given the decreased lymphatic function in obesity, we next investigated basal immune responses in obese mice. Obese mice had a normal ability to produce antibody responses (anti-OVA $IgG_1$ titers) as compared to controls (Figure S3a; p=NS). In contrast, T cells harvested from obese mice and stimulated *ex vivo* using OVA produced significantly less interferon-γ (IFNγ) and interleukin 4 (IL-4) as compared to controls, indicating an impairment in T cell recall (Figure S3b, c; $p<0.01$ and $p<0.05$, respectively). Impaired T cell recall in obese mice was confirmed with *ex vivo* stimulation with 2,4-dinitrobenzenesulfonic acid (DNBS) after *in vivo* sensitization with 1-fluoro-2,4-dinitrobenzene (DNFB) demonstrated significantly less IFNγ production as compared to controls (Figure S3d; $p<0.05$).

## Obese mice have increased contact hypersensitivity

Upon DNFB challenge, obese mice had increased ear erythema, swelling, ear thickness, and epidermal thickness at days 3 and 8 as compared to controls, indicating a more severe inflammatory response (Figure 2a–c, Figure S4a; $p<0.01$ and $p<0.05$, respectively). Flow cytometry analysis of ear tissues harvested from obese mice demonstrated increased numbers of activated T cells ($CD4^+/CD69^+$) (Figure 2d). This correlated with analysis of IFNγ protein levels in ear tissues and serum which showed increased tissue and serum levels of IFNγ in obese mice (Figure 2e, f; $p<0.01$ for all). While lean animals had a 3-fold increase in tissue IFNγ levels, obese mice tissues had a more than 8-fold increase 3 days after DNFB challenge. Similarly, while lean mice had only a mild increase in serum IFNγ levels (∼30%), we noted an almost 2 fold increase in serum levels in obese mice.

Flow cytometry of ear tissues was also performed to analyze T cell subtypes in lean and obese mice after DNFB challenge. These studies demonstrated a nearly 3-fold increase in $CD4^+$ cells, a 7-fold increase in $CD8^+$ cells, a 4-fold increase in T-regulatory cells ($CD4^+/CD25^+$ cells), and a 4-fold increase in macrophages ($CD11b^+/F4/80^+$) (Figure 3a). Histological staining was performed and showed that obese mice have significantly decreased capillary lymphatic vessel density ($LYVE\text{-}1^+$ vessels) both at 3 days (nearly 2-fold decrease) and 8 days (4-fold decrease) after DNFB challenge (Figure 3b, c $p<0.01$ for both). In addition, obese animals had significantly increased generalized inflammation ($CD45^+$ cells) and T cell inflammatory infiltrate ($CD3^+$ cells) at both time points examined, indicating that these mice had increased peak inflammation and delayed clearance of this response (Figure 3d–g; $p<0.05$ for all).

Consistent with our studies with isolated T cells, we found that obese mice also had markedly increased inflammatory responses to a non-specific inflammatory stimulus (croton oil), suggesting that this response is independent from changes in immune cell recall. In these experiments, obese mice treated with croton oil had markedly increased ear thickness and ear weight as compared to controls (Figure S5a–c; $p<0.01$ for both). In addition, similar to our findings with DNFB, we found that obese mice treated with croton oil had increased generalized inflammation ($CD45^+$ cells), $CD3^+$ cell infiltration, and decreased lymphatic vessel density ($LYVE\text{-}1^+$) as compared to controls (Figure S6a–f; $p<0.01$ for CD45 and CD3, $p<0.05$ for LYVE-1). Taken together, our findings suggest that obesity results in impaired lymphatic function, increased basal levels of skin inflammation, and increased immune specific and non-specific inflammatory dermatitis.

## rhVEGF-C improves lymphatic function and decreases contact hypersensitivity

Given that exogenous administration of VEGF-C has been shown to improve lymphatic function in many models of lymphatic insufficiency and dysfunction, we investigated its effect on dermatitis in obesity. Control and obese mice were treated with rhVEGF-C daily, administered subcutaneously in the base of the ear for 7 days and then challenged with DNFB to elicit a contact hypersensitivity response. The rhVEGF-C injections continued for 3 more days post-challenge after which inflammatory responses were analyzed. Evans blue lymphangiography showed that injection of rhVEGF-C increased drainage of interstitial fluid to the collecting lymphatics (white arrows) in both lean and obese mice after DNFB

challenge (Figure 4a). Consistent with this, whole mount staining of ears injected with fluorescently-conjugated tomato lectin revealed uptake of tomato lectin into the collecting lymphatics of the obese mice after rhVEGF-C injection, suggesting that this intervention increased transport of interstitial fluid (Figure 4b). This hypothesis is supported by the finding that rhVEGF-C injections increased trafficking of dendritic cells trafficking from the ear to the cervical lymph nodes in both lean and obese mice after DNFB challenge (Figure 4c; $p<0.05$). Taken together, these findings indicate that VEGF-C treatment in the setting of dermatitis results in improved lymphatic function in both lean and obese mice.

Based on the above findings, we next investigated whether improved lymphatic function in obese mice also decreased dermatitis. Following DNFB challenge, both control and obese mice treated with rhVEGF-C had decreased erythema, swelling, and ear thickness as compared to their respective controls (Figure 5a, b, d, e; $p<0.01$ for all). Whole ear and epidermal thickness measurements in obese mice showed a normalization of these measures and were statistically indistinguishable from baseline values recorded in lean mice with dermatitis.

Treatment of lean and obese mice with rhVEGF-C also markedly increased capillary lymphatic vessel density (LYVE-$1^+$ vessels) but did not alter the number of blood vessels in the ear (Figures 5c, f; S7a–d; $p<0.01$ and p=NS respectively). In addition, although we noted a modest increase in vascular endothelial growth factor receptor (VEGFR)-3 expression by ear skin blood capillaries after DNFB challenge in both lean and obese mice, these effects were not further accentuated by rhVEGF-C administration, suggesting that changes in VEGFR-3 expression that occur in this model are not regulated by VEGF-C (Figure S7a–c). Similarly, consistent with previous reports, we found that although macrophages did not express VEGFR-3 at baseline in either lean or obese mice (data not shown), there was a modest increase in VEGFR-3 expression 3 days following DNFB challenge (Figure S7e**; upper panel**) (Schoppmann *et al*., 2002). However, similar to our findings with blood vessel expression of VEGFR-3, changes in macrophage expression of this receptor were not further modulated by rhVEGF-C administration (Figure S7e**; lower panel**).

In addition, immunohistochemical and immunofluorescence staining of ear tissues demonstrating significantly decreased infiltration of F4/$80^+$, $CD3^+$, and $CD45^+$cells in both lean and obese mice treated with rhVEGF-C as compared with their respective controls (Figure 5g–i, Figure S8a, b; $p<0.01$ for all). Again, similar to our findings with ear thickness and epidermal thickness, we found that the number of these inflammatory cells in ear sections of obese mice normalized back to baseline levels noted in lean mice with dermatitis. Taken together, rhVEGF-C treatment of obese mice leads to increased lymphatic vessel density, improved lymphatic function, and decreased dermatitis as compared to untreated controls.

## rhVEGF-C increases LEC expression of CCL21 and decreases perilymphatic iNOS

To study the cellular mechanisms regulating decreased dendritic cell (DC) trafficking and impaired lymphatic pumping capacity in obese mice, we next analyzed expression of chemokine (C-C motif) ligand 21 (CCL21) using ear whole mount immunofluorescence staining (Figure 6a). Consistent with the known role of CCL21 in regulating DC migration

to lymphatic vessels and our observation that obese animals have impaired trafficking of DCs, we noted a marked decrease in ear lymphatic CCL21 expression of obese mice as compared with lean mice at baseline (Figure 6a**; upper panel**). Similarly, we found that although contact hypersensitivity increased lymphatic vessel CCL21 expression in both lean and obese mice, this increase was blunted in obese mice as compared with lean controls (Figure 6a; middle panel). Finally, consistent with the known role of VEGF-C in regulating CCL21 expression by LECs as well as our observation that rhVEGF-C increased DC trafficking in obese mice, we noted that obese mice treated with subcutaneous rhVEGF-C injections demonstrated marked increases in lymphatic CCL21 expression (Figure 6a**; lower panel**).

Previous studies have shown that inflammatory cell expression of inducible nitric oxide synthase (iNOS) in response to cutaneous inflammatory responses decreases collecting lymphatic pumping capacity (Liao *et al*., 2011). Therefore, to determine if this mechanism contributed to obesity-induced lymphatic dysfunction and increased cutaneous hypersensitivity responses, we localized iNOS expression by macrophages in ear whole mount samples (Figure 6b). Consistent with our finding that obese mice, at baseline, have decreased lymphatic vessel pumping, we found that there is a profound increase in the perilymphatic inflammation and that the majority of these cells express iNOS (Figure 6b**; upper panel**). In addition, lymphatic collectors in obese mice tended to be more dilated than lean controls (Figure 6b**; upper panel**). Three days after the onset of contact hypersensitivity, we noted a marked increase perilymphatic inflammation and iNOS expression in both control and obese mice; however, this response was accentuated in obese animals (Figure 6b**; middle panel**). Similarly, treatment of both lean and obese mice decreased perilymphatic iNOS expression although this response was less pronounced in obese mice (Figure 6b**; lower panel**). Taken together, our results suggest that obesity decreases lymphatic function by multiple mechanisms including generalized decrease in lymphatic vessel density, increased leakage of initial lymphatics, and decreased collecting vessel pumping capacity. These effects are modulated, at least in part, by decreased expression of LEC chemotactic molecules and exogenous expression of iNOS by perilymphatic inflammatory cells.

## Discussion

Contact dermatitis is a common inflammatory skin disease resulting from T cell-mediated delayed type hypersensitivity reactions elicited by skin contact with an irritant in sensitized individuals. The irritant or hapten-laden antigen presenting cells (APCs) from the skin migrate to the draining lymph nodes, where they present the hapten-peptide-MHC complexes to T cells, leading to clonal expansion of specific memory/effector T cells and subsequent recruitment to primary sites of skin contact (Vocanson *et al*., 2005). Upon re-exposure, a robust hapten-specific T cell-mediated inflammatory reaction occurs in the skin (Vocanson *et al*., 2009). However, while it is well known that obesity is associated with increased incidence and severity of atopic and contact dermatitis, the cellular mechanisms that regulate this effect remain poorly understood.

In the current study, we show that similar to the clinical scenario, obese mice exhibit an exaggerated inflammatory response to sensitizing agents (DNFB) and non-specific irritants (croton oil). These responses are characterized by increased peak inflammation and delayed clearance of inflammatory cell infiltrates. In addition, we found that obese mice had profound derangements of their lymphatic system, including decreased lymphatic vessel density, leaky initial lymphatics, and impaired collecting lymphatic pumping capacity. Because the lymphatics play a key role in both antigen and inflammatory cell removal, our findings suggest that obesity-induced lymphatic dysfunction increases dermatitis responses due to the cumulative effect of impaired antigen clearance during the elicitation phase and impaired removal of inflammatory cells post-elicitation. This hypothesis is supported by our finding that improving lymphangiogenesis and lymphatic function markedly decreases inflammatory responses in obese mice. In addition, our hypothesis is supported by previous studies demonstrating that blockade of VEGFR-3 and impaired lymphangiogenesis markedly increases the severity of acute/chronic inflammation in general as well as in chronic hypersensitivity reactions resulting from DNFB exposure in pulmonary and cutaneous models of acute/chronic inflammation (Baluk *et al*., 2005; Huggenberger *et al*., 2010; Kaipainen *et al*., 1995; Kataru *et al*., 2009; Sugaya *et al*., 2012). Thus, targeted treatments designed to augment lymphatic function may represent a novel means of treating inflammatory disorders of the skin.

An interesting finding of our study was that although obese mice had mildly decreased T cell recall responses *ex vivo*, they maintained a normal ability to produce antibodies after vaccination and had exaggerated elicitation responses to antigen stimulation. These findings suggest that although obese mice have impaired lymphatic drainage and trafficking of antigen presenting cells to regional lymph nodes, they have enough capacity to elicit a T cell response upon re-stimulation with an antigen. Therefore, basal increases in cutaneous inflammation and impaired ability to clear antigen/inflammatory cells appear to compensate for mildly impaired T cell recall in obese mice. This hypothesis is supported by previous studies in genetic models of lymphatic dysfunction demonstrating that despite decreased lymphatic transport function and impaired antigen cell trafficking to draining lymph nodes during the sensitization phase, mice with congenital abnormalities of the lymphatic system are still capable of activating efficient T cell responses (Platt *et al*., 2013).

Previous studies have shown that T cells are crucial regulators of pathologic responses to obesity, including metabolic syndrome and cancer (Nishimura *et al*., 2009; Wu *et al*., 2007). For example, depletion studies have shown that T cell inflammatory responses are necessary for infiltration of macrophages and regulate insulin sensitivity (Nishimura *et al*., 2009; Winer *et al*., 2009). In addition, our lab and others have shown that T cells exert potent anti-lymphangiogenic effects and that functional lymphatics are necessary for clearance of T cell inflammatory responses (Kataru *et al*., 2011; Zampell *et al*., 2012). Thus, it is possible that obesity-induced T cell inflammation exerts anti-lymphangiogenic effects resulting in decreased lymphatic vessel density and impaired removal/clearance of T cell inflammatory responses in sensitized individuals.

The microenvironment secondary to high fat diet may also contribute to the observed lymphatic dysfunction seen in obesity. Previous studies have shown that inflamed

adipocytes can release adipokines such as IL-6 and TNF-α, as well as substances such as free fatty acids that have direct effects on surrounding tissues (Hajer *et al*., 2008). Specifically, stearic acid and palmitic acid have been shown to stimulate the TLR-4 inflammatory signaling cascade associated with obesity (Davis *et al*., 2008; Shi *et al*., 2006; Suganami *et al*., 2007). Whether or not these pathways have a direct effect on lymphatic impairment or are altered due to local injections of VEGF-C will require additional study.

Previous studies, in contrast to our findings, have suggested that obese mice have impaired contact hypersensitivity responses as compared to lean mice (Katagiri *et al*., 2007). This discrepancy is likely related to technical differences and varying definitions of obesity used between our studies. For example, some studies used only short periods of high fat diet exposure (1–2 weeks in one study or as long as 37 days in another) while in our current study, consistent with previously published reports on diet-induced obesity in mice, animals were maintained on a high fat diet for much longer periods of time (10–12 weeks). As a result, obese mice in our study were nearly 25g heavier (or double the body weight) than lean controls. In contrast, the aforementioned study recorded maximum weight gains of only 4g compared to their lean controls. This is important since we have found that obesity-induced lymphatic dysfunction is not typically measurable unless the total body weight is greater than 45g (unpublished results). This finding is supported by previous clinical studies in overweight patients, suggesting that a body mass index threshold of 59 is necessary for spontaneous development of lower extremity lymphedema (Greene *et al*., 2012). Thus, direct comparison of our study with previous reports on obesity and dermatologic inflammation is difficult since mice treated in the latter studies likely did not meet the weight threshold to exhibit lymphatic dysfunction.

Consistent with previous studies, we found that delivery of VEGF-C markedly increased lymphangiogenesis and improved lymphatic function (Szuba *et al*., 2002; Yoon *et al*., 2003). In addition, we found that VEGF-C injections increased cutaneous lymphatic endothelial cell (LEC) expression of CCL21 and decreased iNOS accumulation around collecting lymphatic vessels which provide potential mechanisms for decreased contact hypersensitivity through improved immune cell trafficking in *both* lean and obese mice. Importantly, we found the effect of VEGF-C to be specific to the lymphatic vessels as we did not observe obesity related differences in blood vessel counts or changes in VEGFR-3 expression on blood vessels or macrophages after VEGF-C treatment. The findings that VEGF-C injections decrease inflammation in obese animals is consistent with previous studies in lean mice demonstrating that subcutaneous injection of recombinant VEGF-C156S protein in K14-VEGF-A transgenic mice (a model of chronic skin inflammation) decreases ear swelling and inflammation (Huggenberger *et al*., 2010). Other studies in lean mice using adenoviral transfer of VEGF-C/blockade of VEGF-R3 with neutralizing antibodies or transgenic over-expression of VEGF-C in the skin (K14-VEGF-C), have also shown that the VEGF-C-VEGFR3 signaling pathway plays an important role in the resolution of skin inflammation and that increased lymphatic density accelerates this process (Hagura *et al*., 2014; Kataru *et al*., 2009). In an interesting clinical study, Cliff *et al*. found that patients with plaque psoriasis have proliferation of lymphatic vessels surrounding the plaque but decreased numbers of lymphatic vessels within the plaque (Cliff *et al*., 1999).

Furthermore, vessels within the plaque had impaired lymphatic uptake, suggesting that impaired lymphatic function may contribute to the pathology of plaque psoriasis. Taken together, our findings in the context of previous reports in the literature support the hypothesis that dermal lymphatics play a key role in the resolution of inflammatory responses and that dysfunction of these networks in obesity promotes exaggerated hypersensitivity reactions.

## Methods

### Diet-induced obesity

All experimental protocols were reviewed and approved by the Institutional Animal Care and Use Committee (IACUC) at Memorial Sloan Kettering Cancer Center. Six week old male C57BL/6J (Jackson Laboratories, Bar Harbor, Maine) mice were fed either a high fat diet (60% kcal from fat; W.F Fisher & Son, Inc., NJ) or a normal chow diet (13% Kcal from fat; Purina PicoLab Rodent Diet 20, W.F. Fisher & Son) *ad libitum* for 10–12 weeks (Nishimura *et al*., 2009; Weitman *et al*., 2013). At the conclusion of the experiment, animals were weighed using a digital scale (Sartorius, Bradford, MA).

### Analysis of lymphatic function

Lymphangiography using Evans blue dye (2 μl of 1% (wt/vol)) (Sigma-Aldrich, St. Louis, MO) was used to identify leaky lymphatic vessels and analyze lymphatic architecture (Jang *et al*., 2013). Functional lymphatic vessel staining was performed by injecting tomato lectin (1 mg/ml; Sigma-Aldrich) in the apex of the ear, followed by sacrifice 10 minutes later, as described previously (Nishimura *et al*., 2009). All experiments were performed with a minimal of 5 animals per group.

Near-infrared (NIR) imaging was performed using a modification of the methods reported previously (Nelson *et al*., 2014; Weiler and Dixon, 2013; Weiler *et al*., 2012). Briefly, animals were anesthetized with 2% isoflurane and placed on a heating pad after depilation. The field of view was adjusted to capture the entire tail and left hind limb. NIR probes were made using previously established protocols for conjugating IRDye 800 CW (LI-COR Biotechnology, Lincoln, NE) to a 40 kDa polyethylene glycol molecule (PEG) (JenKem Technology USA Inc., Allen, TX) (Proulx *et al*., 2013). 10μL of the NIR probe was injected intradermally at the tip of the tail or in the footpad of the hind limb. NIR images of dynamic fluorescence transport were captured for 10 minutes at 10 fps and a 50 ms exposure time. Image processing of the 10 minute image sets were used to determine the fluorescence packet frequency. Fluorescence intensity within regions of interest (ROIs) was drawn and tracked using a custom LabVIEW virtual interface. The lymphatic packet frequency was determined to be the number of distinct fluorescence packets passing through the ROIs on the lymphatic vessels per minute.

The rate of lymphatic fluid transport from peripheral tissues to the systemic circulation was analyzed using FITC-conjugated dextran (2,000 kDa, 10 mg/ml, Invitrogen, Grand Island, NY) injected bilaterally into the forepaw under controlled pressure followed by analysis of

signal intensity in the serum (IVIS 200 optical imaging system; Xenogen Corp, Alameda, CA).

### Immunization and T cell recall

Mice were immunized intradermally in each hind limb (40 μl/injection) and tail (20 μl) with 0.1mg/ml chicken OVA (Bachem, Torrance, CA) in a 1:1 emulsion of PBS and alum (Thermo Scientific, Waltham, MA) followed by a booster 10 days later as described previously (Thomas *et al., 2012*). Antibody titers in the serum were analyzed 21 days after immunization using an enzyme-linked immunosorbant assay (ELISA; Alpha Diagnostic International, San Antonio, TX). In addition, the draining lymph nodes (popliteal, sciatic, and sacral) and spleen were harvested and digested to form cell suspensions, plated, and then stimulated with 5 mg/ml OVA (Bachem, Torrance, CA dissolved in RPMI). 5 days later, cell supernatants were harvested and IFN-γ, and IL-4 cytokine production was analyzed by ELISA (eBioscience, San Diego, CA), according to the manufacturer's protocol.

T cell recall was performed similarly with DNBS. Briefly, DNFB (25 μl of 0.5% DNFB solution; Toronto Research Chemicals Inc., Toronto, Ontario) was mixed in acetone with 20% olive oil and painted onto the shaved abdomens of mice. 5 days later, spleens and draining lymph nodes were harvested. T cells were isolated from spleens and lymph nodes using positive selection CD3 magnetic beads (Miltenyi Biotec, Cambridge, MA) as per the manufacturer's recommendations and were subsequently plated and then stimulated with 50μM DNBS (Sigma-Aldrich) for 5 days after which conditioned media was collected and IFN-γ cytokine production was analyzed by ELISA (eBioscience, San Diego, CA), according to the manufacturer's protocol.

### Model of contact hypersensitivity

To establish contact hypersensitivity, we used a modified previously described technique (Martin-Romero *et al*., 2000). 25 μl of 0.5% DNFB (Toronto Research Chemicals Inc., Toronto, Ontario) in acetone with 20% olive oil was painted onto the shaved abdomens of mice. Five days later, one ear was challenged with 0.3% DNFB. Histological ear swelling was measured at 3 and 8 days post-challenge.

### Model of non-specific inflammation

To determine if obese mice had prolonged resolution and clearance of non-specific inflammation, we used a well-described croton oil assay (Sugaya *et al*., 2012). 20 μl of 2% croton oil (Sigma-Aldrich) dissolved in 70% acetone (Fisher Scientific, Pittsburgh, PA) was painted onto the inner ear surface followed by analysis 18 hours later.

### rhVEGF-C therapy and dendritic cell trafficking

1μl of rhVEGF-C (0.1mg/ml, R&D, Minneapolis, MN) was injected intradermally with a Hamilton syringe into the base of the ear in obese and lean animals every day for 7 days prior to induction of contact hypersensitivity and for 3 days post-challenge for a total of 10 days (Szuba *et al*., 2002). Control animals were injected with 1μl of sterile PBS. To quantify dendritic cell (DC) trafficking, we used a modification of previously reported methods (Lim

*et al*., 2009). Briefly, the spleens of CD45.1 B6.SJL-*Ptprca Pepcb*/BoyJ mice (Jackson Laboratories) were harvested and digested with collagenase D (Sigma-Aldrich). $CD45.1^+$ DCs were enriched using a magnetic microbead-based positive selection kit for $CD11c^+$ cells (Miltenyi Biotech, Gladbach, Germany). Isolated cells were resuspended in PBS and injected into the apex of the right ear ($10^6$ cells per injection), and 18 hours later the right cervical lymph nodes were harvested and analyzed for migrating DCs ($CD45.1^+/CD11c^+/MHC\text{-}II^{high}$) using flow cytometry (LSRII;BD Biosciences, San Jose, CA) and FlowJo software (Tree Star, Ashland, OR). Each experiment was repeated with 4–5 animals per group.

## Supplementary Material

Refer to Web version on PubMed Central for supplementary material.

## Acknowledgments

**Source of Funding:** NIH R01 HL111130-01 awarded to BJM.

The authors are grateful to Mesruh Turkekul, Sho Fujisawa, and Yevgeniy Romin of the Molecular Cytology Core at Memorial Sloan Kettering Cancer Center for assistance with both histology and tissue imaging (Core Grant (P30 CA008748)).

## References

Arngrim N, Simonsen L, Holst JJ, et al. Reduced adipose tissue lymphatic drainage of macromolecules in obese subjects: a possible link between obesity and local tissue inflammation? Int J Obes (Lond). 2013; 37:748–750. [PubMed: 22751255]

Baluk P, Tammela T, Ator E, et al. Pathogenesis of persistent lymphatic vessel hyperplasia in chronic airway inflammation. J Clin Invest. 2005; 115:247–257. [PubMed: 15668734]

Blum KS, Karaman S, Proulx ST, et al. Chronic high-fat diet impairs collecting lymphatic vessel function in mice. PLoS One. 2014; 9:e94713. [PubMed: 24714646]

Cliff S, Bedlow AJ, Stanton AW, et al. An in vivo study of the microlymphatics in psoriasis using fluorescence microlymphography. Br J Dermatol. 1999; 140:61–66. [PubMed: 10215769]

Davis JE, Gabler NK, Walker-Daniels J, et al. Tlr-4 deficiency selectively protects against obesity induced by diets high in saturated fat. Obesity. 2008; 16:1248–1255. [PubMed: 18421279]

Garfinkel L. Overweight and cancer. Annals of internal medicine. 1985; 103:1034–1036. [PubMed: 4062120]

Gerdes S, Rostami-Yazdi M, Mrowietz U. Adipokines and psoriasis. Experimental dermatology. 2011; 20:81–87. [PubMed: 21255085]

Glass CK, Olefsky JM. Inflammation and lipid signaling in the etiology of insulin resistance. Cell metabolism. 2012; 15:635–645. [PubMed: 22560216]

Greene AK, Grant FD, Slavin SA. Lower-extremity lymphedema and elevated body-mass index. The New England journal of medicine. 2012; 366:2136–2137. [PubMed: 22646649]

Gregor MF, Hotamisligil GS. Inflammatory mechanisms in obesity. Annu Rev Immunol. 2011; 29:415–445. [PubMed: 21219177]

Hagura A, Asai J, Maruyama K, et al. The VEGF-C/VEGFR3 signaling pathway contributes to resolving chronic skin inflammation by activating lymphatic vessel function. J Dermatol Sci. 2014; 73:135–141. [PubMed: 24252749]

Hajer GR, van Haeften TW, Visseren FL. Adipose tissue dysfunction in obesity, diabetes, and vascular diseases. European heart journal. 2008; 29:2959–2971. [PubMed: 18775919]

Hamminga EA, van der Lely AJ, Neumann HA, et al. Chronic inflammation in psoriasis and obesity: implications for therapy. Medical hypotheses. 2006; 67:768–773. [PubMed: 16781085]

Harvey NL, Srinivasan RS, Dillard ME, et al. Lymphatic vascular defects promoted by Prox1 haploinsufficiency cause adult-onset obesity. Nat Genet. 2005; 37:1072–1081. [PubMed: 16170315]

Huggenberger R, Ullmann S, Proulx ST, et al. Stimulation of lymphangiogenesis via VEGFR-3 inhibits chronic skin inflammation. J Exp Med. 2010; 207:2255–2269. [PubMed: 20837699]

Jang JY, Koh YJ, Lee SH, et al. Conditional ablation of LYVE-1+ cells unveils defensive roles of lymphatic vessels in intestine and lymph nodes. Blood. 2013; 122:2151–2161. [PubMed: 23836558]

Kaipainen A, Korhonen J, Mustonen T, et al. Expression of the fms-like tyrosine kinase 4 gene becomes restricted to lymphatic endothelium during development. Proc Natl Acad Sci U S A. 1995; 92:3566–3570. [PubMed: 7724599]

Katagiri K, Arakawa S, Kurahashi R, et al. Impaired contact hypersensitivity in diet-induced obese mice. J Dermatol Sci. 2007; 46:117–126. [PubMed: 17350227]

Kataru RP, Jung K, Jang C, et al. Critical role of CD11b+ macrophages and VEGF in inflammatory lymphangiogenesis, antigen clearance, and inflammation resolution. Blood. 2009; 113:5650–5659. [PubMed: 19346498]

Kataru RP, Kim H, Jang C, et al. T lymphocytes negatively regulate lymph node lymphatic vessel formation. Immunity. 2011; 34:96–107. [PubMed: 21256057]

Lavie CJ, Milani RV, Ventura HO. Obesity and cardiovascular disease: risk factor, paradox, and impact of weight loss. Journal of the American College of Cardiology. 2009; 53:1925–1932. [PubMed: 19460605]

Liao S, Cheng G, Conner DA, et al. Impaired lymphatic contraction associated with immunosuppression. Proc Natl Acad Sci U S A. 2011; 108:18784–18789. [PubMed: 22065738]

Lim HY, Rutkowski JM, Helft J, et al. Hypercholesterolemic mice exhibit lymphatic vessel dysfunction and degeneration. Am J Pathol. 2009; 175:1328–1337. [PubMed: 19679879]

Lim HY, Thiam CH, Yeo KP, et al. Lymphatic vessels are essential for the removal of cholesterol from peripheral tissues by SR-BI-mediated transport of HDL. Cell metabolism. 2013; 17:671–684. [PubMed: 23663736]

Lumeng CN, Saltiel AR. Inflammatory links between obesity and metabolic disease. J Clin Invest. 2011; 121:2111–2117. [PubMed: 21633179]

Marino MG, Carboni I, De Felice C, et al. Risk factors for psoriasis: a retrospective study on 501 outpatients clinical records. Annali di igiene : medicina preventiva e di comunita. 2004; 16:753–758. [PubMed: 15697005]

Martin-Romero C, Santos-Alvarez J, Goberna R, et al. Human leptin enhances activation and proliferation of human circulating T lymphocytes. Cellular immunology. 2000; 199:15–24. [PubMed: 10675271]

Mokdad AH, Ford ES, Bowman BA, et al. Prevalence of obesity, diabetes, and obesity-related health risk factors, 2001. Jama. 2003; 289:76–79. [PubMed: 12503980]

Nelson TS, Akin RE, Weiler MJ, et al. Minimally invasive method for determining the effective lymphatic pumping pressure in rats using near-infrared imaging. American journal of physiology Regulatory, integrative and comparative physiology. 2014; 306:R281–R290.

Nishimura S, Manabe I, Nagasaki M, et al. CD8+ effector T cells contribute to macrophage recruitment and adipose tissue inflammation in obesity. Nat Med. 2009; 15:914–920. [PubMed: 19633658]

Ogden CL, Carroll MD, Flegal KM. Prevalence of obesity in the United States. Jama. 2014; 312:189–190. [PubMed: 25005661]

Perez-Hernandez AI, Catalan V, Gomez-Ambrosi J, et al. Mechanisms linking excess adiposity and carcinogenesis promotion. Front Endocrinol (Lausanne). 2014 May 1.5:65. [PubMed: 24829560]

Platt AM, Rutkowski JM, Martel C, et al. Normal dendritic cell mobilization to lymph nodes under conditions of severe lymphatic hypoplasia. J Immunol. 2013; 190:4608–4620. [PubMed: 23530147]

Proulx ST, Luciani P, Alitalo A, et al. Non-invasive dynamic near-infrared imaging and quantification of vascular leakage in vivo. Angiogenesis. 2013; 16:525–540. [PubMed: 23325334]

Rutkowski JM, Markhus CE, Gyenge CC, et al. Dermal collagen and lipid deposition correlate with tissue swelling and hydraulic conductivity in murine primary lymphedema. Am J Pathol. 2010; 176:1122–1129. [PubMed: 20110415]

Savetsky IL, Torrisi JS, Cuzzone DA, et al. Obesity increases inflammation and impairs lymphatic function in a mouse model of lymphedema. Am J Physiol Heart Circ Physiol. 2014; 307:H165–H172. [PubMed: 24858842]

Schoppmann SF, Birner P, Stockl J, et al. Tumor-associated macrophages express lymphatic endothelial growth factors and are related to peritumoral lymphangiogenesis. Am J Pathol. 2002; 161:947–956. [PubMed: 12213723]

Shi H, Kokoeva MV, Inouye K, et al. TLR4 links innate immunity and fatty acid-induced insulin resistance. The Journal of clinical investigation. 2006; 116:3015–3025. [PubMed: 17053832]

Silverberg JI, Kleiman E, Lev-Tov H, et al. Association between obesity and atopic dermatitis in childhood: a case-control study. J Allergy Clin Immunol. 2011; 127:1180–1186. e1. [PubMed: 21411132]

Silverberg JI, Silverberg NB, Lee-Wong M. Association between atopic dermatitis and obesity in adulthood. Br J Dermatol. 2012; 166:498–504. [PubMed: 21999468]

Suganami T, Tanimoto-Koyama K, Nishida J, et al. Role of the Toll-like receptor 4/NF-kappaB pathway in saturated fatty acid-induced inflammatory changes in the interaction between adipocytes and macrophages. Arteriosclerosis, thrombosis, and vascular biology. 2007; 27:84–91.

Sugaya M, Kuwano Y, Suga H, et al. Lymphatic dysfunction impairs antigen-specific immunization, but augments tissue swelling following contact with allergens. J Invest Dermatol. 2012; 132:667–676. [PubMed: 22071476]

Szuba A, Skobe M, Karkkainen MJ, et al. Therapeutic lymphangiogenesis with human recombinant VEGF-C. Faseb J. 2002; 16:1985–1987. [PubMed: 12397087]

Thomas SN, Rutkowski JM, Pasquier M, et al. Impaired humoral immunity and tolerance in K14-VEGFR-3-Ig mice that lack dermal lymphatic drainage. J Immunol. 2012; 189:2181–2190. [PubMed: 22844119]

Vocanson M, Hennino A, Chavagnac C, et al. Contribution of CD4(+ )and CD8(+) T-cells in contact hypersensitivity and allergic contact dermatitis. Expert review of clinical immunology. 2005; 1:75–86. [PubMed: 20477656]

Vocanson M, Hennino A, Rozieres A, et al. Effector and regulatory mechanisms in allergic contact dermatitis. Allergy. 2009; 64:1699–1714. [PubMed: 19839974]

Weiler M, Dixon JB. Differential transport function of lymphatic vessels in the rat tail model and the long-term effects of Indocyanine Green as assessed with near-infrared imaging. Frontiers in physiology. 2013; 4:215. [PubMed: 23966950]

Weiler M, Kassis T, Dixon JB. Sensitivity analysis of near-infrared functional lymphatic imaging. Journal of biomedical optics. 2012; 17:066019. [PubMed: 22734775]

Weitman ES, Aschen SZ, Farias-Eisner G, et al. Obesity impairs lymphatic fluid transport and dendritic cell migration to lymph nodes. PLoS One. 2013; 8:e70703. [PubMed: 23950984]

Winer S, Chan Y, Paltser G, et al. Normalization of obesity-associated insulin resistance through immunotherapy. Nat Med. 2009; 15:921–929. [PubMed: 19633657]

Wu H, Ghosh S, Perrard XD, et al. T-cell accumulation and regulated on activation, normal T cell expressed and secreted upregulation in adipose tissue in obesity. Circulation. 2007; 115:1029–1038. [PubMed: 17296858]

Yoon YS, Murayama T, Gravereaux E, et al. VEGF-C gene therapy augments postnatal lymphangiogenesis and ameliorates secondary lymphedema. J Clin Invest. 2003; 111:717–725. [PubMed: 12618526]

Zampell JC, Avraham T, Yoder N, et al. Lymphatic function is regulated by a coordinated expression of lymphangiogenic and anti-lymphangiogenic cytokines. Am J Physiol Cell Physiol. 2012; 302:C392–C404. [PubMed: 21940662]

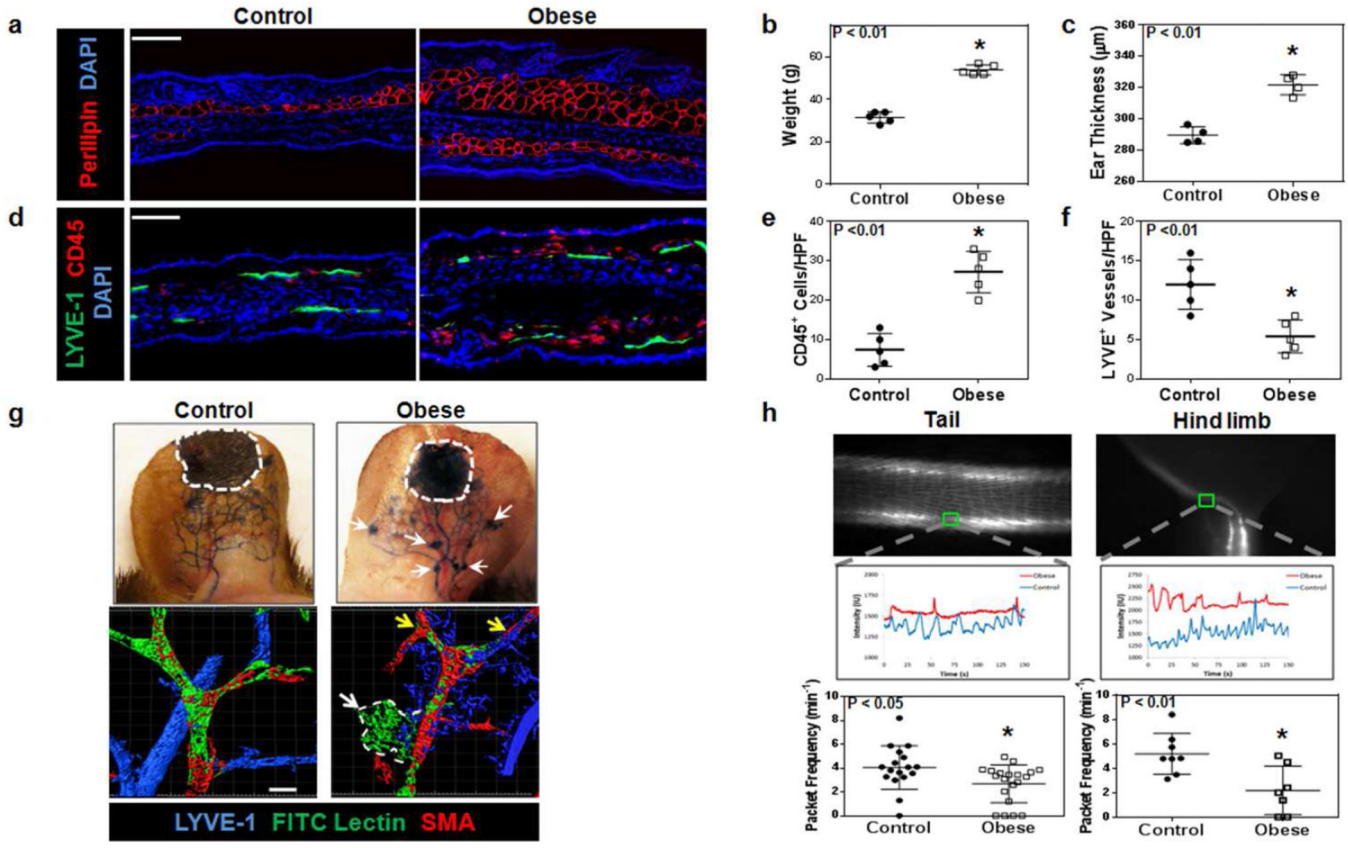


**Figure 1. Obese mice have impaired lymphatic function at baseline**

**a.** Representative baseline immunofluorescence images of perilipin staining from ear cross-sections of control (i.e. lean) and obese mice. Scale bar=50μm.

**b.** Body weights of control and obese mice (n=5 each; *p<0.01).

**c.** Baseline ear thickness of control and obese mice (n=5 animals/group; *p<0.01).

**d.** Representative baseline immunofluorescence images of ear cross-sections from control and obese mice stained for LYVE-1 (green), CD45 (red), and DAPI (blue). Scale bar=50μm.

**e.** Cell counts of $CD45^+$ cells/high power field (HPF) in ear cross-sections of control and obese mice. Cell counts were performed at 100x magnification in a minimum of 3 sections per mouse and 4–5 mice/group.

**f.** Lymphatic vessel density ($LYVE\text{-}1^+$ vessels/HPF) in control and obese mice.

**g.** Top: Evans blue lymphangiography of ear skin in control and obese mice at baseline. Outlined area represents injection site. Arrows indicate leakage of dye from lymphatic vessels. Bottom: Representative ear whole mount images of FITC lectin lymphangiography from control and obese mice. Note decreased lymphatic uptake (yellow arrows) and extra-lymphatic leakage (dotted white line) of FITC lectin from $\alpha\text{-SMA}^+$ collecting lymphatics in obese mice. Scale bar=50μm.

**h.** Top: Representative NIR imaging of lymphatic vessels in the tail and hind limb. Middle: Representative graphs for NIR imaging demonstrating collecting lymphatic vessel contraction (control = blue, obese = red) in the tail and hind limb of control and obese mice. Bottom: Quantification of packet frequency in the tail (n=5–8 mice/group; *p<0.05) and hind limb (n=5–8 mice/group; *p<0.01) of control and obese mice.

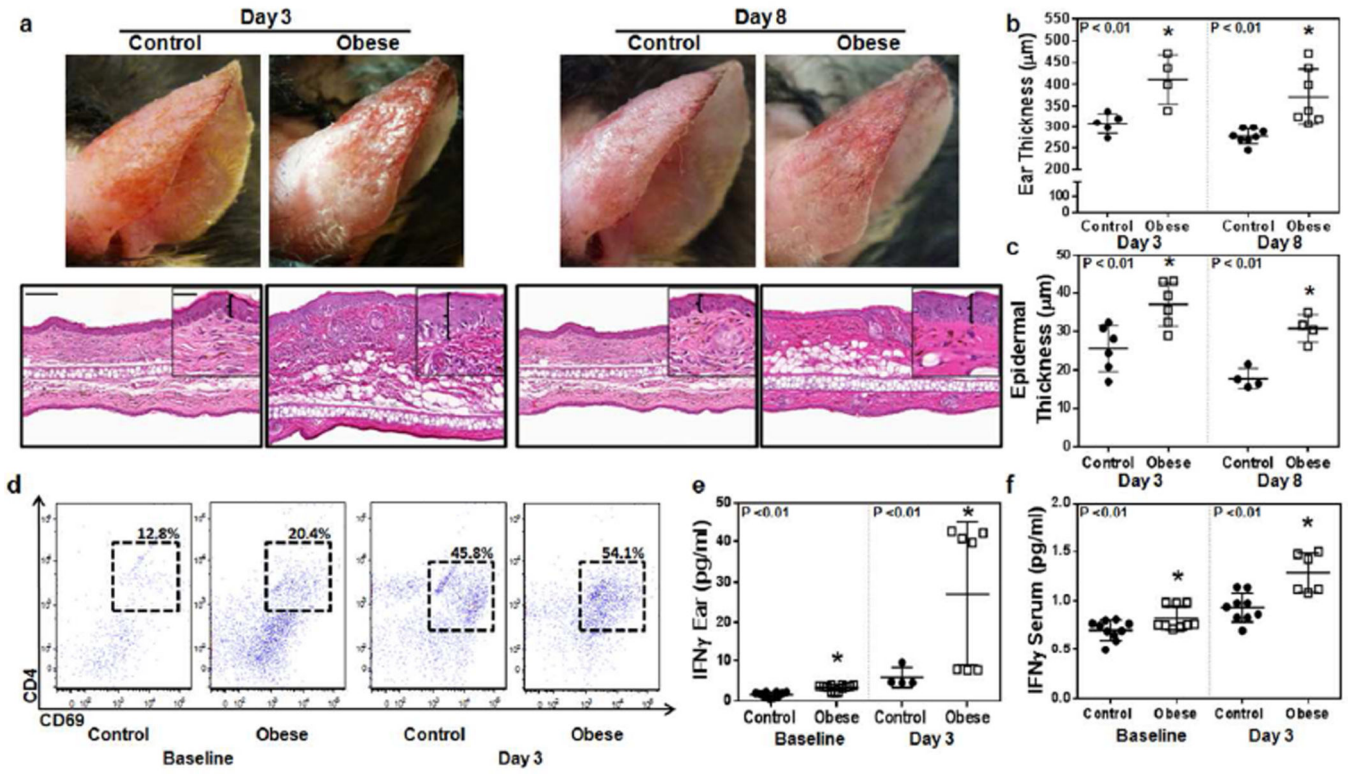


**Figure 2. Obese mice have increased contact hypersensitivity**

**a.** Top: Representative gross images of control and obese mice ears shown 3 and 8 days after challenge with DNFB. Bottom: Representative histology of ear skin sections of control and obese mice 3 and 8 after challenge with DNFB. Low-power (5x, scale bar=100μm) and high-power (20×, scale bar=50μm). Brackets in high-power images demonstrate epidermal ear thickness.

**b.** Quantification of ear thickness in control and obese mice 3 and 8 days after DNFB challenge (n=5–8 animals/group; *p<0.01).

**c.** Quantification of epidermal thickness in control and obese mice 3 and 8 days after DNFB challenge (n=5–8 animals/group; *p<0.01).

**d.** Representative dot plots of ear skin flow cytometry at baseline and 3 days after challenge with DNFB analyzing activated T-helper cells ($CD3^+/CD69^+/CD4^+$).

**e.** Quantification of ear tissue IFNγ protein concentration in control and obese mice at baseline and 3 days following DNFB challenge (n=5 animals/group *p<0.01).

**f.** Quantification of serum IFNγ protein concentration in control and obese mice at baseline and 3 days following DNFB challenge (n=5–8 animals/group; *p<0.01).

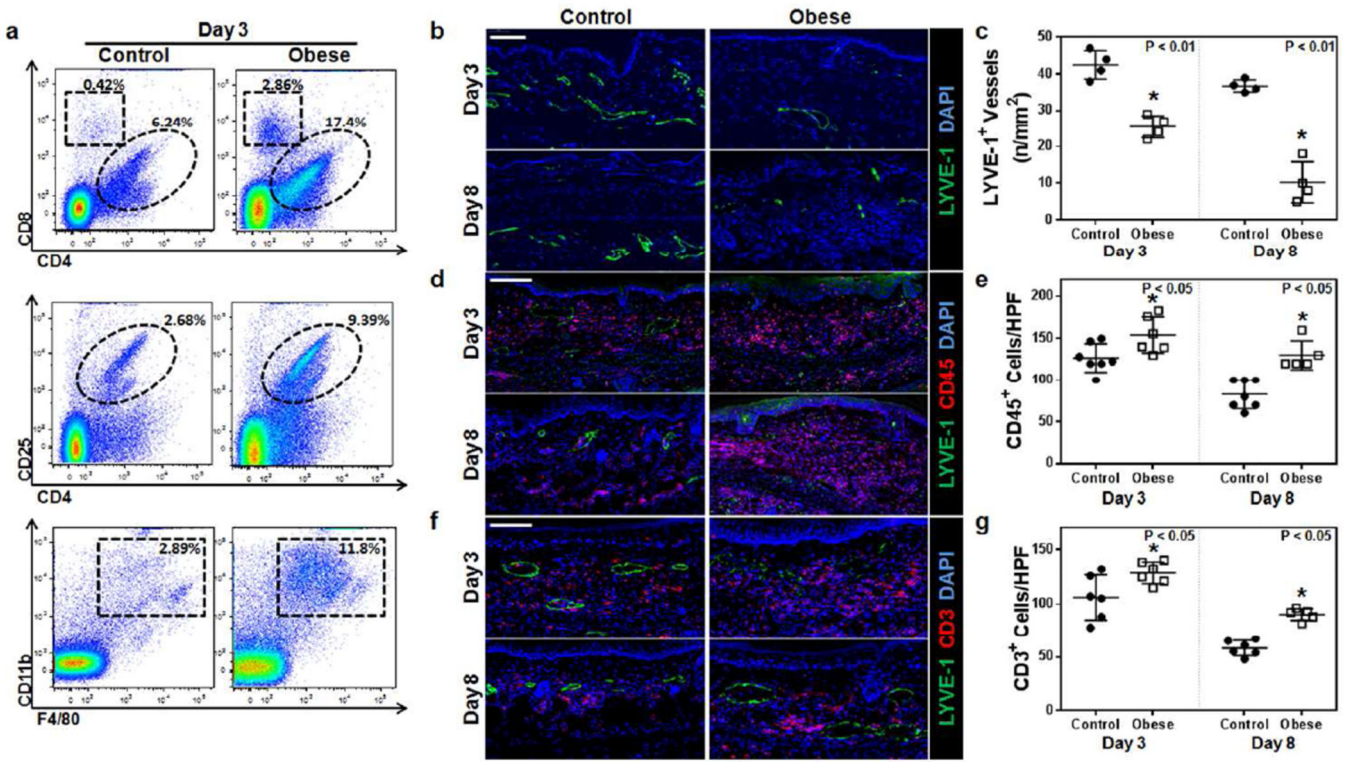


**Figure 3. Obesity decreases clearance of contact hypersensitivity-induced inflammation**

**a.** Representative flow plots analyzing control and obese mouse ears 3 days after DNFB challenge. Top: T-helper ($CD3^+/CD4^+$) and cytotoxic T cells ($CD3^+/CD8^+$); Middle: T-regulatory cells ($CD3^+/CD4^+/CD25^+$); Bottom: macrophages ($CD11b^+/F4/80^+$).

**b, c.** Representative immunofluorescence localization (**b**) and quantification (**c**) of LYVE-$1^+$ vessels (green) in ear skin cross-sections harvested from control and obese mice 3 or 8 days following DNFB challenge (n= 5–6 each; *p<0.01). Blue stain is DAPI. Scale bar=100μm.

**d, e.** Representative immunofluorescence localization (**d**) and quantification (**e**) of $CD45^+$ cells (red) and LYVE-$1^+$ vessels (green) in ear skin cross-sections harvested from control and obese mice 3 or 8 days following DNFB challenge (n=5–10 each; *p<0.05). Blue stain is DAPI. Scale bar=100μm.

**f, g.** Representative immunofluorescence localization (**f**) and quantification (**g**) of $CD3^+$ cells (red) and LYVE-$1^+$ vessels (green) in ear skin cross-sections harvested from control and obese mice 3 or 8 days following DNFB challenge (n=5–10 each; *p<0.05). Blue stain is DAPI. Scale bar=100μm.

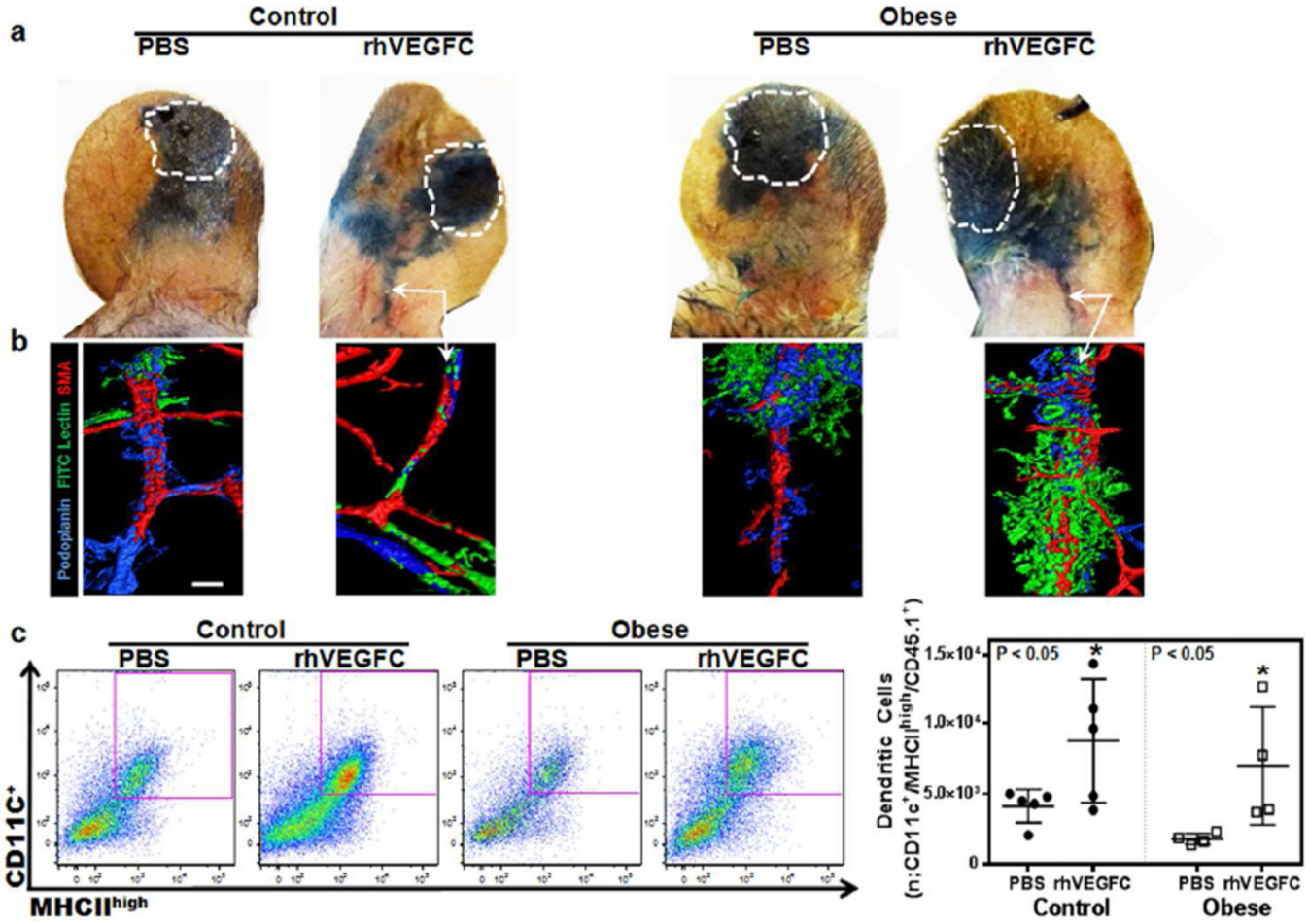


**Figure 4. Subcutaneous injection of rhVEGF-C in ear skin improves lymphatic function and decreases contact hypersensitivity in both lean and obese mice**

**a.** Evans blue lymphangiography of control and obese mouse ears 3 days after DNFB challenge. Mice were injected in the base of the ear with either PBS or rhVEGF-C subcutaneously once daily for 7 days and then challenged with DNFB. Subsequently, PBS and rhVEGF-C injections were continued for an additional 3 days post-challenge after which lymphangiography was performed. White dashed line area represents Evans blue injection site. Arrows show dye in collecting lymphatic vessels at the base of the ear in control and obese mice injected with rhVEGF-C.

**b.** Representative ear whole mount images of FITC lectin lymphangiography of control and obese mouse ears 3 days following DNFB challenge in animals treated with daily PBS or rhVEGF-C injections for 10 days as outlined above. White arrows show functional lymphatic vessels containing intraluminal tomato lectin stain (green) in rhVEGF-C treated lean and obese mice groups. Scale bar=50μm.

**c.** Left panel: Representative flow cytometry plots of dendritic cells ($CD11c^+/MHCII^{high}/CD45.1^+$) harvested from cervical lymph nodes draining the ipsilateral ears of DNFB challenged control and obese mice treated with daily ear subcutaneous PBS or rhVEGF-C injections (7 days before and 3 days after DNFB challenge). Purple box represents positive cells. Right panel: Quantification of the migrated DCs from ear skin to draining lymph

nodes in various groups (n=5 animals/group; *p<0.05). Note increased DC trafficking in lean and obese mice injected with rhVEGF-C.

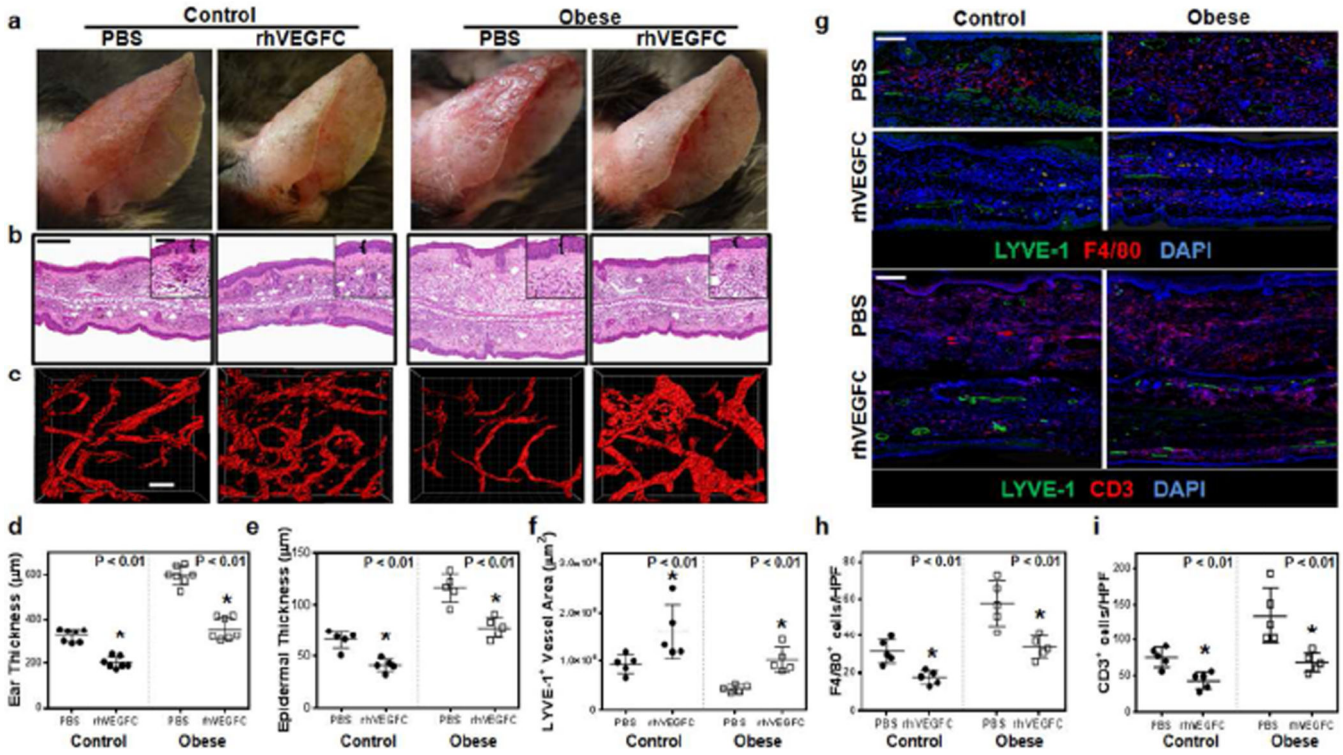


**Figure 5. Improving lymphatic function in obese mice with rhVEGF-C decreases contact hypersensitivity**

**a.** Representative gross images of control and obese mice 3 days following DNFB challenge. Mice were treated with daily ear subcutaneous injections of PBS or rhVEGF-C (7 days before and 3 days after DNFB challenge). Note decreased gross inflammatory response in both lean and obese mice treated with rhVEGF-C.

**b.** Representative low and high power (boxed areas) histological cross sections of control and obese mouse ears shown in Figure 5a. Brackets in high-power images demonstrate epidermal ear thickness. Scale bar=100μm (low power) and 50μm (high power).

**c.** Representative immunofluorescence localization of LYVE-1$^+$ vessels in ear whole mount images of control and obese mouse ears shown in Figure 5a. Note increased lymphatic vessel density in rhVEGF-C treated animals. Scale bar=100μm.

**d. e.** Quantification of ear thickness (**d**) and epidermal thickness (**e**) of animal groups described in Figure 5b (n=5–8 animals/group; *p<0.01).

**f.** Lymphatic vessel areas (LYVE-1$^+$ vessels) in control and obese mice treated with PBS or rhVEGF-C and harvested 3 days following DNFB challenge.

**g.** Representative immunofluorescence localization of macrophages (upper panels; F4/80$^+$ cells shown in red) and T cells (lower panels; CD3$^+$ cells shown in red) in control and obese mice treated with PBS or rhVEGF-C and harvested 3 days following DNFB challenge. Lymphatic vessels (LYVE-1$^+$) are shown in green in both panels. Scale bar=100μm.

**h, i.** Quantification of macrophages (F4/80$^+$ cells/HPF; **h**) and T cells (CD3$^+$ cells/HPF; **i**) in control and obese mice treated with PBS or rhVEGF-C and harvested 3 days following DNFB challenge (n= 3 HPF/animal and 5 animals/group; *p<0.01).

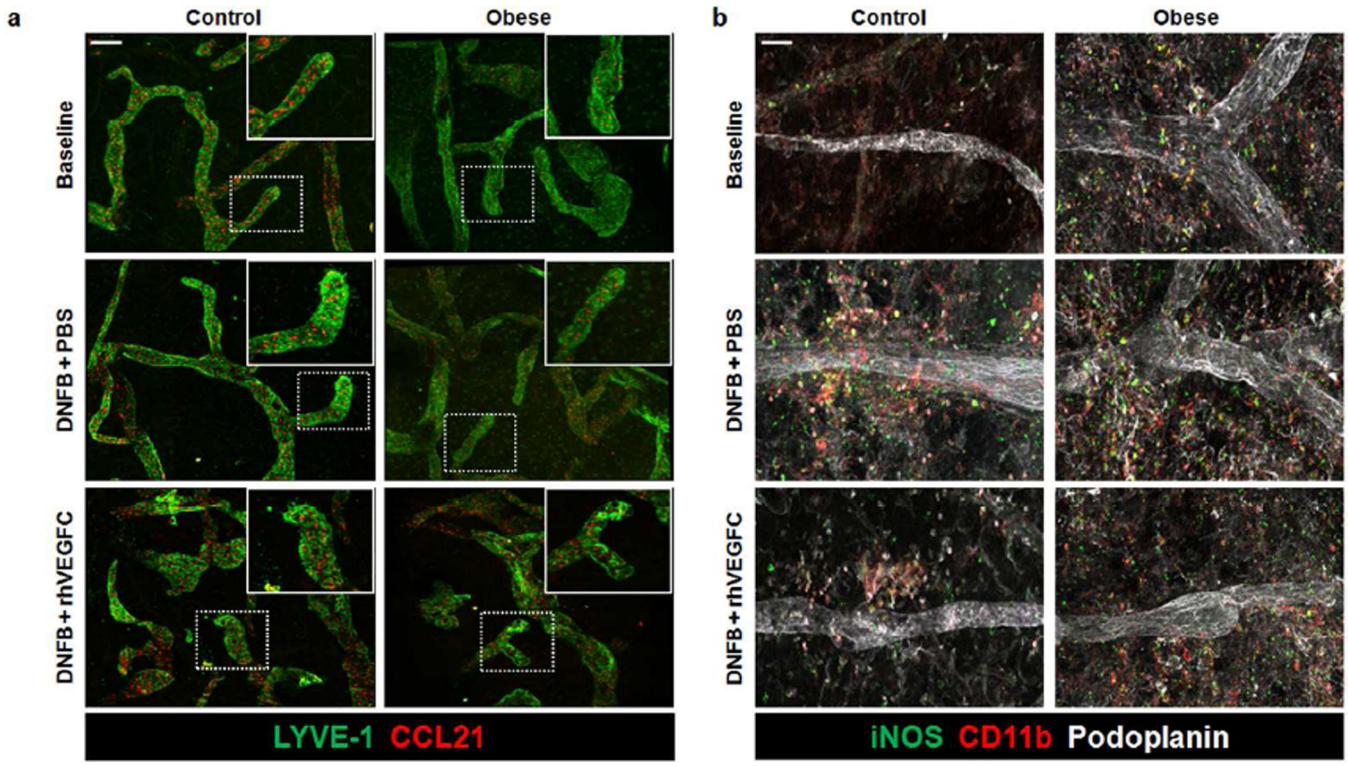


**Figure 6. rhVEGF-C increases LEC expression of CCL21 and decreases perilymphatic iNOS$^+$ macrophages**

**a.** Representative low and high power (dashed box shown in upper right inset) immunofluorescence images of ear whole mounts localizing CCL21 (red) and lymphatic vessels (LYVE-1$^+$; green) in control and obese mice. Top: Represents before DNFB challenge (baseline). Middle: Represents 3 days after DNFB challenge + daily intradermal PBS injections (DNFB+PBS). Bottom: Represents 3 days after DNFB challenge + daily intradermal rhVEGF-C injections (DNFB + rhVEGF-C). PBS and rhVEGF-C injections were administered for 7 days before and 3 days after DNFB challenge. Scale bar=50μm.

**b.** Representative immunofluorescence images of ear whole mounts localizing iNOS (green), macrophages (CD11b$^+$; red), and lymphatic vessels (podoplanin$^+$; white) in control and obese animals as described in Figure 6a. Top: baseline images (i.e. no DNFB, no injections). Middle: 3 days after DNFB challenge with pre/post challenge subcutaneous PBS injections; Bottom: 3 days after DNFB challenge with pre/post challenge subcutaneous rhVEGF-C injections. Scale bar=50μm.